Installation Effects on the Capacity of Open-Ended and Closed-Ended Pipe Piles

Monica Prezzi, Venkata Abhishek Sakleshpur, and Daniel G. Fridman

Abstract The base and shaft capacities of piles depend on the method of pile installation, pile type, soil type, and stress state. Fully instrumented, open-ended, and closed-ended pipe piles were load tested side-by-side statically following a slow-maintained testing protocol at two sites in Indiana, USA. The piles were instrumented following a hybrid, dense instrumentation scheme with both vibrating-wire and electrical-resistance strain gauges along the entire length of the shafts. The open-ended piles were specially designed and assembled following a double-wall system to facilitate separation of the external and internal unit shaft resistances in every layer of the soil profile. The plug length ratio (PLR) and incremental filling ratio (IFR) were measured for the open-ended test piles. To gain insights on the impact of the formation and evolution of the soil plug during installation on the base capacity of pipe piles, one open-ended model pile and one closed-ended model pile were installed under similar conditions in a calibration chamber with digital image capabilities. This paper summarizes and discusses the results of the pile load tests. The load test results are compared with predictions obtained using modern CPT-based pile design methods available in the literature. An assessment of the design methods is made based on the field test results.

Keywords Pile load test · Open-ended pile · Closed-ended pile · DIC

1 Introduction

Piles are generally categorized as non-displacement or displacement piles, depending on the installation method. A closed-ended pipe pile (CEP) is a displacement pile, whereas the response of an open-ended pipe pile (OEP) typically lies between that of a displacement and a non-displacement pile [1]. A soil plug develops inside an OEP during installation [2], and the plug length L_p may be less than or equal to the

M. Prezzi (✉) · V. A. Sakleshpur · D. G. Fridman
Lyles School of Civil Engineering, Purdue University, West Lafayette, IN 47907, USA
e-mail: mprezzi@ecn.purdue.edu

B. Indraratna and C. Rujikiatkamjorn (eds.), *Recent Advances and Innovative Developments in Transportation Geotechnics*,
https://doi.org/10.1007/978-981-97-8245-1_2

pile penetration depth L. If $L_p = L$, the pile is driven in an unplugged/fully coring mode throughout, whereas if $L_p < L$, the pile is driven in a partially or fully plugged mode at least during part of the installation [3]. In general, when comparing the response of pipe piles of the same geometry installed in the same soil profile, an OEP driven in a fully coring mode would have a load response that is stiffer than that of a non-displacement pile, whereas an OEP driven in a fully plugged mode would have a load response that approaches that of a CEP [4].

Side-by-side field static load tests (SLTs) on fully instrumented CEPs and OEPs installed in the same soil profile allow us to study the effects of pile installation on the pile shaft and base capacities. Calibration chamber tests with image-capturing capabilities provide the means to systematically study the response of pipe piles during installation and loading under controlled conditions. This paper summarizes the results of side-by-side SLTs performed on full-scale, instrumented CEPs and OEPs at two sites in Indiana, USA. The test results are compared with predictions obtained using modern CPT-based pile design methods. We also present preliminary results of a model OEP and a model CEP tested in the digital image correlation (DIC) calibration chamber at Purdue University. The effects of pile installation are reflected in the measured displacement fields in the soil domain surrounding the model piles.

2 Pile Load Tests in Indiana

2.1 Lagrange County

A CEP and an OEP were tested side-by-side at a bridge construction site over the Pigeon River in Lagrange County, Indiana [5, 6]. The soil profile consists of gravelly sand (Table 1); the top 3 m is in a loose state ($D_R \approx 30\%$), while the rest of the deposit is in a dense-to-very dense state ($D_R \approx 80\%$), with SPT blow counts ranging from 20 to 60, and cone resistance q_c values, from 15 to 25 MPa. The water table is at 3 m depth below the ground surface.

The wall thickness t and outer diameter B of the CEP are equal to 12.7 and 356 mm. The double-wall OEP was assembled by combining an inner pipe with B = 305 mm and an outer pipe with B = 356 mm; both pipes had the same value of

Table 1 Soil layers at the pile load test site in Lagrange County, Indiana [5, 6]

z (m)	Layer description	γ_m (kN/m^3)	e_{min} (–)	e_{max} (–)	D_R (%)	ϕ_c (°)
0–3	Gravelly sand	16.38	0.41	0.68	30	33.3
3–13	Gravelly sand	21.20	0.41	0.68	80	33.3

Note z = depth below ground surface, e_{min} = minimum void ratio, γ_m = unit weight, e_{max} = maximum void ratio, ϕ_c = critical-state friction angle, and D_R = relative density

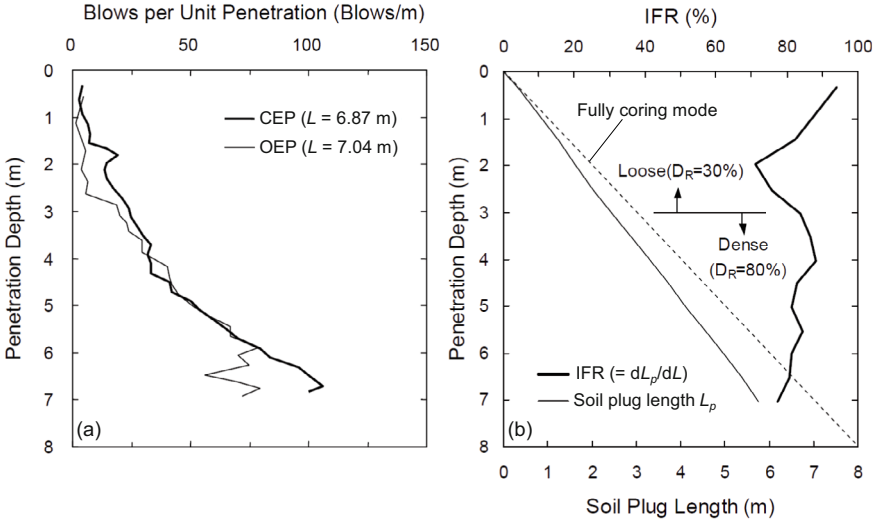

Fig. 1 Pile driving results for the Lagrange County site (modified after [5]): **a** driving resistance (blow counts) of CEP and OEP, and **b** IFR and soil plug length for the OEP

t (= 6.4 mm). The spacing between the OEP and the CEP was about 4.9 m. Nine pairs of electrical-resistance (ER) strain gauges were installed on the CEP, while the inner and outer pipes of the OEP were instrumented with ten pairs and nine pairs of ER strain gauges, respectively.

The CEP and the OEP were driven to depths of 6.87 and 7.04 m (Fig. 1a). Figure 1b shows that the OEP was partially plugged and never reached a fully plugged state (with IFR = 0; IFR = dL_p/dL). The values of PLR (= L_p/L) and IFR at the end of OEP driving were 0.82 and 0.78. Measurements of soil plug length recorded before and after the SLT showed that the soil plug length did not change as a result of the SLT, indicating that either the OEP behaved as a fully plugged pile under static loading, or any compression of the soil plug was likely compensated by soil entering the pile from the bottom during loading.

2.2 *Tippecanoe County*

A CEP and an OEP were tested side-by-side at a bridge construction site over the Wabash River in Tippecanoe County, Indiana [7, 8]. The soil profile at the site generally consists of layers of poorly graded sand with different gravel contents (Table 2). The gravel content was small (< 20%) for depths less than 15 m, except for a narrow layer at around 9 m depth, where the gravel content exceeded 50%. The

gravel content ranged from 30 to 60% for depths exceeding 15 m. The water table was found at a depth of 3.05 m below the ground surface. Additional site investigation results are reported in [7, 8].

The wall thickness t and outer diameter B of the CEP are equal to 13 and 610 mm. The OEP was composed of a bottom segment and a top segment (each 18.3 m long). The bottom double-wall segment consists of an inner pipe with $B = 584$ mm and an outer pipe with $B = 660$ mm; both pipes had the same value of t (= 13 mm). The outer diameter of the bottom and top segments of the OEP were the same, but the value of t for the top segment was 19 mm. The spacing between the OEP and the CEP was about 7.3 m.

The shaft of the CEP was instrumented with 20 pairs of ER and 12 pairs of vibrating-wire (VW) strain gauges [9, 10]. For the double-wall OEP, 19 pairs of ER gauges were installed along the inner pipe of the bottom segment, whereas 11 and 14 pairs of VW and ER gauges were installed along the outer pipe of the bottom segment [11]. In addition, the top segment of the OEP was instrumented with three and five pairs of VW and ER gauges, respectively [12]. Further information about the CEP and OEP instrumentation is reported in the literature [9–12].

The CEP was driven to a depth of 17.37 m below the ground surface (Fig. 2a). For installation of the OEP, a 0.9 m-diameter steel casing was first installed up to a depth of 8.53 m, the soil inside the casing was excavated, and then the OEP was driven to a depth of 30.48 m below the ground surface. Figure 2b shows that the IFR decreased from 0.92 to 0.70 during installation of the OEP, and that the PLR was approximately 0.78 at the end of driving of the OEP. The OEP and the CEP were load tested 8 days and 13 days, respectively, after pile driving.

Table 2 Soil layers at the pile load test site in Tippecanoe County, Indiana [7, 8]

z (m)	Layer description	γ_m (kN/m^3)	D_{50} (mm)	GC (%)	C_U (–)	ϕ_c (°)	δ_c (°)
0.0–5.5	Clayey silt with sand	19.5	–	0	3.0	30	24.6
5.5–8.2	Sand with gravel	20.0	0.4	4	2.6	32	26.2
8.2–10.4	Sandy gravel	21.5	4.5	49	34.6	35	23.1
10.4–16.8	Sand with gravel	20.0	0.9	10	4.8	32	24.3
16.8–22.6	Gravelly sand	21.5	4.1	43	16.6	34	23.1
22.6–32.6	Gravelly sand	21.5	1.1	28	8.3	33	25.1

Note z = depth below ground surface, D_{50} = mean particle size, γ_m = unit weight, GC = gravel content (= percent of soil particles by mass retained on the 4.75 mm sieve), ϕ_c = critical-state friction angle, C_U = coefficient of uniformity, and δ_c = critical-state interface friction angle

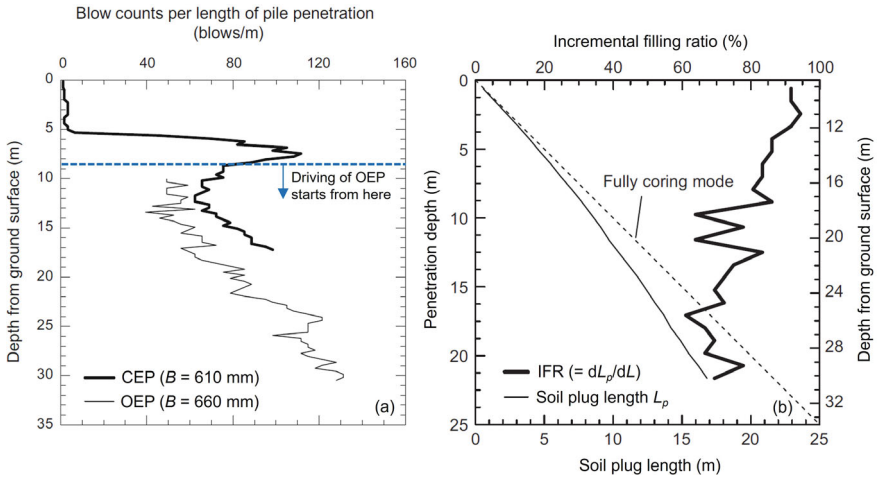

Fig. 2 Pile driving results for Tippecanoe County site: **a** comparison between driving resistances of CEP and OEP (after [7]), and **b** soil plug length and IFR for OEP (after [11])

3 Comparison Between Predicted and Measured Resistances

Several CPT-based methods have been proposed to predict the ultimate load capacity of CEPs and OEPs in sand [13–16]. Some of these methods include the Purdue Pile Design Method (PPDM) [7, 17], the Unified Pile Design Method (UPDM) [18], and the Imperial College Pile Design Method (ICPDM) [19].

Figure 3 compares the predicted and measured axial load transfer curves at the ultimate load level (when $w = 0.1B$) for the instrumented CEPs and OEPs tested in Indiana; w = pile head settlement. The axial load transfer curve for the OEP in Lagrange County was not included in Fig. 3 because some of the gauges in the lower part of the outer pipe malfunctioned after pile driving [5]. The PPDM, ICPDM, and UPDM provided good estimates of the base and shaft capacities of the CEP in Lagrange County (Fig. 3a). For the CEP in Tippecanoe County, all three methods estimated the limit shaft capacity Q_{sL} quite well—the PPDM, ICPDM, and UPDM provided estimates of Q_{sL} that were within ± 10% of the measured value, with the ICPDM just 5% below the measured shaft capacity. However, the methods overpredicted the ultimate base capacity $Q_{b,ult}$ of the CEP due to the high gravel content (= 50%) found at the pile base level, resulting in a large q_c value (= 28.7 MPa, averaged from $1B$ above to $2B$ below the pile base) for use in the pile base capacity calculations. The ICPDM provided the closest estimate of $Q_{b,ult}$ (= 1.5 times the measured base capacity) for the CEP in Tippecanoe County (Fig. 3b). For the OEP in Tippecanoe County, we see the opposite trend, where all three methods predicted the pile base capacity reasonably well—the PPDM, ICPDM, and UPDM provided estimates of $Q_{b,ult}$ that were within − 12% of the measured value, with the PPDM

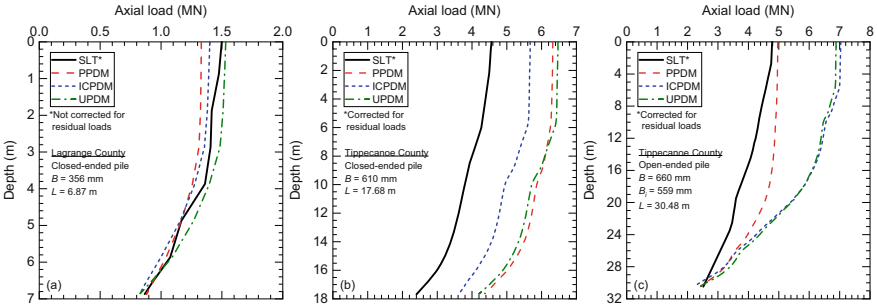

Fig. 3 Predicted and measured axial load transfer curves at the ultimate load level for **a** CEP in Lagrange County, **b** CEP in Tippecanoe County, and **c** OEP in Tippecanoe County

just 3% below the measured base capacity, even though the gravel content at the level of the OEP base was 28%. This is because: (1) the annulus thickness of the OEP (= 51 mm) was comparable to the cone diameter d_c (= 44.5 mm), resulting in a cone resistance that was representative of the resistance mobilized by the pile annulus, and (2) the measured annulus resistance Q_{ann} was approximately 88% of the base resistance $Q_{b,ult}$ of the OEP at the ultimate load level. While the PPDM predicted the limit shaft capacity of the OEP quite well, both the ICPDM and UPDM overpredicted Q_{sL} by a factor of two (Fig. 3c). A layer-by-layer comparison of the predicted and measured limit unit shaft resistance q_{sL} profiles in Tippecanoe County indicates that the overestimation of q_{sL} for the CPT-based methods occurred at depths where the gravel content was higher than 30% [7, 11]. Although the gravel content was not reported for the Lagrange County test site, the fairly good match between the measured and predicted axial load transfer curves suggests that the gravel content at this site was probably low (< 30%).

In practice, when detailed site characterization is unavailable, engineers often rely on parameters c_s (= q_{sL}/q_c) and β (= q_{sL}/σ'_{v0}) to calculate the outer unit shaft resistance q_{sL} of pipe piles in sand; σ'_{v0} = in situ vertical effective stress at the elevation where q_{sL} is computed. Figure 4 shows the values of c_s and β determined from the SLT results at the ultimate load level for the instrumented CEPs and OEPs in Indiana. For both test sites, the values of c_s and β are generally higher for the CEP than the OEP; this is likely because of the displacement of a greater volume of the surrounding soil by the driving of CEPs than OEPs, resulting in a higher degree of soil densification and lateral stress increase around the shaft of the CEPs. The c_s and β values determined from the SLT data generally agree with the range of values documented in the literature (c_s = 0.1–0.9% and β = 0.3–0.9 for driven piles in sand [1, 17, 20]).

Figure 4 also shows the values of the lateral earth pressure coefficient K mobilized within the depth range of the active plug length for the instrumented OEPs in Indiana. The magnitude and distribution of K_{inner} and K_{outer}, which are the values of K (= q_{sL}/

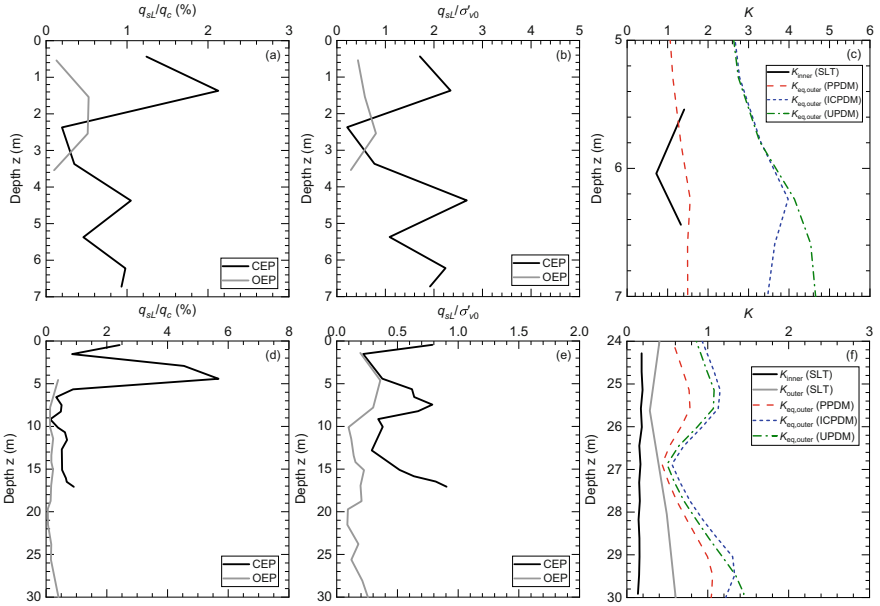

Fig. 4 Profiles of c_s ($= q_{sL}/q_c$), β ($= q_{sL}/\sigma'_{v0}$), and K ($= q_{sL}/\sigma'_{v0} \tan \delta_c$) for pipe piles installed in gravelly sand deposits in Lagrange County (**a**–**c**) and Tippecanoe County (**d**–**f**)

$\sigma'_{v0} \tan \delta_c$) mobilized along the inner and outer pipes of the double-wall OEPs, were determined at the ultimate load level from the strain gauges installed on the surfaces of the inner and outer pipes. The value of K_{inner} was determined by assuming that the vertical effective stress σ'_v inside the plug is equal to the value of σ'_{v0} outside the pile at the elevation of interest. For the CPT-based design methods, the magnitude and distribution of $K_{eq,outer}$, which is the equivalent K mobilized along the outer pipe of the OEP, was estimated from the method equations; for example, $K_{eq,outer} = K(1 - 0.66PLR)$ for the PPDM, and $K_{eq,outer} = (\sigma'_{rc} + \Delta\sigma'_{rd})/\sigma'_{v0}$ for both the ICPDM and UPDM (using the expressions for K, σ'_{rc}, and $\Delta\sigma'_{rd}$ as defined in the methods). Figure 4c shows that, for the OEP in Lagrange County, the value of K_{inner} is approximately equal to 1.0, on average, while the values of $K_{eq,outer}$ range from 1.0 to 4.6, with smaller values corresponding to the PPDM. Similarly, Fig. 4f shows that, for the OEP in Tippecanoe County, the values of K_{inner} and K_{outer} range from about 0.14 to 0.16 and 0.3 to 0.6, while the values of $K_{eq,outer}$ range from 0.4 to 1.4, with smaller values corresponding to the PPDM. The values of K_{inner} from the SLT are approximately constant within the active plug length for the OEP in Tippecanoe County. The active plug length $L_{p,A}$ at the ultimate load level is approximately equal to 7 and 11 inner diameters for the OEPs in Lagrange County and Tippecanoe County, respectively. The ratio $L_{p,A}/L_p$ of the active plug length to the total plug length (measured at the end of driving) was comparable for the OEPs at both test sites (= 35 and 38% for Lagrange and Tippecanoe Counties).

For the OEP in Tippecanoe County, the value of β inside the plug was calculated at the ultimate load level by assuming that σ'_v inside the plug is equal to σ'_{v0} outside the pile at the elevation of interest. This is a practical approach because, in design, the vertical effective stresses inside the plug are unknown. Following this approach, the values of β obtained from the SLT along the active plug length range from about 0.06 to 0.08. Using the formulation derived in [21], which assumes that β is constant along the active plug length, we calculated a value of β equal to 0.05 by assuming that the vertical effective stress at the base of the plug is equal to the unit plug resistance q_{plug} (= 1.3 MPa) obtained from the SLT at the ultimate load level. For OEPs driven under partially plugged conditions, the practical approach of using σ'_{v0} is convenient in the calculation of unit plug resistance, and β values within the above range may be used as reference for OEPs installed in soil profiles similar to that at the Tippecanoe County test site. Note that, for smaller values of IFR, with driving approaching fully plugged conditions, the β values may vary along the active plug length. In the formulation of [21], the vertical effective stresses in the soil plug increase exponentially near the pile base, but this change in the vertical effective stress may be due in part to these varying β values. Calibration chamber test data indicate that the transfer of load in the soil plug tends to increase significantly near the pile base [2, 22]. Another factor in the experimental determination of β values inside the plug is the separation of the annulus resistance from the plug resistance based on discrete instrumentation within the inner pipe wall.

Table 3 summarizes the measured and predicted values of the normalized ultimate unit base resistance c_b (= $q_{b,ult}/q_{cb}$) for the instrumented CEPs and OEPs tested in gravelly sand profiles in Indiana; q_{cb} = representative cone resistance at the pile base level. For the SLT $q_{b,ult}/q_{cb}$ ratios, the value of q_{cb} was calculated by taking the average of the q_c values over a distance of 1B above and 2B below the pile base. For Lagrange County, the CPT-based methods predict values of c_b that are in good agreement with those measured from the SLTs for both the CEP and OEP. For Tippecanoe County, the predicted and measured c_b values agree closely with each other for the OEP but not for the CEP (for the reasons mentioned previously). Given that the limit unit base resistance q_{bL} (at plunging) of a CEP, particularly one that has a conical tip (as is the case for the CEP tested in Tippecanoe County), is generally comparable to the cone resistance measured near the pile base [17], the values of c_b were recalculated assuming q_{cb} to be equal to q_{bL} (= 10.4 MPa, measured in the SLT on the CEP). The values of c_b estimated from the CPT-based design methods, assuming $q_{cb} = q_{bL}$, tend to be closer to the measured value (= 0.79), except for the UPDM, where c_b is always equal to 0.50 for CEPs in sand. The unit plug resistance q_{plug} and the unit annulus resistance q_{ann} of the OEP in Tippecanoe County at the ultimate load level were 6 and 93% of q_{cb} (= 22.8 MPa, averaged 1B above and 2B below the pile base).

Table 3 Predicted and measured values of c_b ($= q_{b,ult}/q_{cb}$) for CEPs and OEPs tested in Indiana

Test/design method	$q_{b,ult}/q_{cb}$ [Lagrange]		$q_{b,ult}/q_{cb}$ [Tippecanoe]		
	CEP	OEP	CEP[b]	CEP[c]	OEP
SLT ($w = 0.1B$)	0.55[a]	0.35[a]	0.29	0.79	0.32
PPDM	0.56	0.28	0.52	0.77	0.31
ICPDM	0.50	0.33	0.43	1.00	0.28
UPDM	0.50	0.30	0.50	0.50	0.31

[a] Not corrected for residual loads (due to drifts in the zero readings of the strain gauges)
[b] Based on q_{cb} calculated using the CPT data
[c] Based on q_{cb} assumed as equal to q_{bL} (= 10.4 MPa) measured from the SLT

4 DIC-Based Calibration Chamber Tests

The digital image correlation (DIC) technique can be used to obtain the displacement and strain fields in the soil domain around model footings [23–26] and model cones/piles [27–37] tested in calibration chambers with image capabilities. The DIC chamber at Purdue University is a half-cylindrical calibration chamber with observation windows positioned on its plane of symmetry. All boundaries of the chamber are fixed-wall boundaries, except the top surface of the soil sample, where a vertical stress (surcharge) can be applied. Additional details about the chamber and the DIC technique can be found in [27]. Tests were performed on a model OEP and CEP installed in uniform dense samples ($D_R \approx 90\%$) of Ottawa 20–30 (OTC) sand (a clean silica sand with $D_{50} = 0.72$ mm and $\phi_c = 29.3°$). The steel model OEP has an outer diameter of 50.8 mm and a wall thickness of 9.5 mm, while the conical-tip brass model CEP has a diameter of 38.1 mm.

The sand samples were air-pluviated inside the chamber, and the top surface of the sand was carefully leveled to facilitate application of the vertical stress using an inflatable air bladder. For both the model CEP and OEP tests, the vertical stress at the center of the second observation window (end of the test) was approximately 40 kPa. The model CEP and OEP were preinstalled 50 and 140 mm into the sand sample (before application of the surcharge) to ensure pile alignment and prevent sand intrusion between the observation window and the model pile. The piles were monotonically jacked into the sand at a rate of 1 mm/s. During the experiments, digital images of the sand domain were captured by two 12-megapixel monochrome cameras. The IFR values measured during penetration of the model OEP were in the range of 0.7–0.9, with a slight decrease in IFR with increasing pile penetration depth L.

Figure 5 shows the radial displacement du_r and vertical displacement du_z fields obtained for the model CEP and OEP in dense OTC sand. The DIC analyses correspond to 234 mm of pile penetration, from $L = 140$ mm (reference image) to $L = 374$ mm (end of test); the figure axes are normalized with respect to the pile radius r_p. The displacement fields for both the model CEP and OEP have a similar pattern, in the sense that vertical displacements dominate within the zone immediately below the pile base, while radial displacements dominate within the zone radially adjacent to the pile shafts. The radial displacement contours extend further into the sand domain for the model OEP than the CEP, with the 1.5 mm du_r contour, for example, reaching a vertical distance of $4r_p$ below the OEP base and a radial distance of $7r_p$ from the OEP centerline (Fig. 5a). A similar trend can also be observed for the vertical displacement fields; for example, the 2 mm du_z contour for the model OEP extends beyond a vertical distance of $5r_p$ below the pile base and up to a radial distance of $5r_p$ from the pile centerline (Fig. 5c). For the model CEP, the 2 mm du_z contour extends up to a vertical distance of $3.5r_p$ below the pile base and a radial distance of approximately $3r_p$ from the pile centerline (Fig. 5d). Despite the relatively high IFR values measured for the OEP, the model OEP produced greater overall soil displacements than the CEP, likely because of its larger diameter.

5 Conclusions

The paper summarizes two case histories of static load tests on fully instrumented, closed-ended pipe piles (CEPs) and double-wall open-ended pipe piles (OEPs) tested side-by-side in gravelly sand deposits in Indiana. Three CPT-based pile design methods were used to predict the axial load transfer curves of the test piles. Profiles of commonly used design parameters c_s, β, and K were developed from the SLT results; these profiles may be used as reference for calculation of unit shaft resistances of CEPs and OEPs installed in similar soil profiles. From the SLT results, the values of K mobilized along the inner pipe of the OEP at the ultimate limit state were compared with those mobilized along the outer pipe as well as those predicted by the design methods. The results of DIC-based calibration chamber tests on model CEPs and OEPs highlight the effects of pile installation on the magnitude and extent of the vertical and radial displacement fields in the soil domain around the model piles; these differences directly affect the load-transfer behavior and load-carrying capacity of these piles.

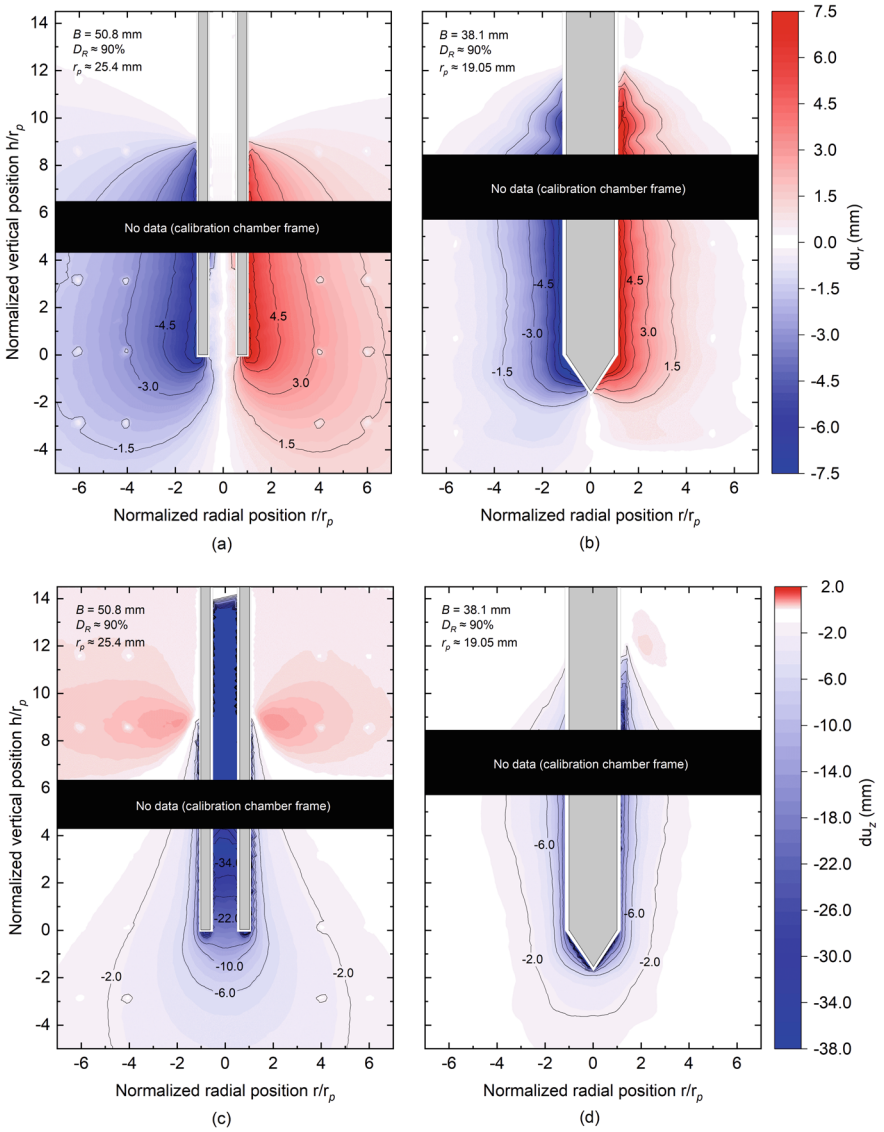

Fig. 5 DIC results for the model OEP and CEP in dense OTC sand showing the radial displacement fields (**a**, **b**) and the vertical displacement fields (**c**, **d**)

Acknowledgements The work related to the field pile load tests was funded by the Joint Transportation Research Program administered by the Indiana Department of Transportation and Purdue University through Contracts SPR-2361 and SPR-4040. The DIC calibration chamber research work was funded by the National Science Foundation under Grant No. 2028672. Any opinions, findings, and conclusions or recommendations expressed in this material are those of the author(s) and do not necessarily reflect the views of the National Science Foundation.

References

1. Lee J, Salgado R, Paik K (2003) Estimation of load capacity of pipe piles in sand based on cone penetration test results. J Geotech Geoenviron Eng 129(5):391–403
2. Paik K-H, Lee S-R (1993) Behavior of soil plugs in open-ended model piles driven into sands. Mar Georesour Geotechnol 11(4):353–373
3. Paik K, Salgado R (2003) Determination of bearing capacity of open-ended piles in sand. J Geotech Geoenviron Eng 129(1):46–57
4. De Nicola A, Randolph MF (1997) The plugging behaviour of driven and jacked piles in sand. Géotechnique 47(4):841–856
5. Paik K, Salgado R, Lee J, Kim B (2003) Behavior of open- and closed-ended piles driven into sands. J Geotech Geoenviron Eng 129(4):296–306
6. Kim K, Salgado R, Lee J, Paik K (2002) Load tests on pipe piles for development of CPT-based design method. JTRP publication no. FHWA/IN/JTRP-2002/04. Purdue University
7. Han F, Ganju E, Salgado R, Prezzi M (2019) Comparison of the load response of closed-ended and open-ended pipe piles driven in gravelly sand. Acta Geotech 14:1785–1803
8. Han F, Ganju E, Salgado R, Prezzi M, Zaheer M (2019) Experimental study of the load response of large diameter closed-ended and open-ended pipe piles installed in alluvial soil. JTRP publication no. FHWA/IN/JTRP-2019/03. Purdue University, West Lafayette, IN, USA
9. Ganju E, Han F, Prezzi M, Salgado R (2020) Static capacity of closed-ended pipe pile driven in gravelly sand. J Geotech Geoenviron Eng 146(4):04020008
10. Ganju E, Han F, Prezzi M, Salgado R (2021) The axial capacity of closed-ended pipe piles driven in gravelly sands. In: Proceedings of IFCEE. Dallas, TX, USA, pp 377–387
11. Han F, Ganju E, Prezzi M, Salgado R, Zaheer M (2020) Axial resistance of open-ended pipe pile driven in gravelly sand. Géotechnique 70(2):138–152
12. Han F, Ganju E, Salgado R, Prezzi M (2020) Static load test on open-ended pipe pile using double-wall instrumentation. In: Proceedings of geo-congress 2020. Minneapolis, pp 73–81
13. Sakleshpur VA, Prezzi M, Salgado R, Zaheer M (2021) CPT-based geotechnical design manual, volume 2: CPT-based design of foundations (methods). JTRP publication no. FHWA/IN/JTRP-2021/23. Purdue University, West Lafayette, IN, USA
14. Sakleshpur VA, Prezzi M, Salgado R, Zaheer M (2021) CPT-based geotechnical design manual, volume 3: CPT-based design of foundations (example problems). JTRP publication no. FHWA/IN/JTRP-2021/24. Purdue University, West Lafayette, IN, USA
15. Prezzi M, Sakleshpur VA (2022) Static and dynamic testing and design methods for driven piles in multilayered soil. In: Proceedings of 11th international conference on stress wave theory and design and testing methods for deep foundations. Rotterdam, pp 1–14
16. Sakleshpur VA, Prezzi M, Salgado R (2023) CPT-based design of pile foundations in sand and clay: perspectives. In: Proceedings of 8th international symposium on deformation characteristics of geomaterials. Porto, Portugal, pp 1–8
17. Salgado R (2022) The engineering of foundations, slopes and retaining structures, 2nd edn. CRC Press, Boca Raton, FL, USA
18. Lehane B, Liu Z, Bittar E, Nadim F, Lacasse S, Jardine R, Carotenuto P, Rattley M, Jeanjean P, Gavin K, Gilbert R, Bergan-Haavik J, Morgan N (2020) A new "unified" CPT-based axial pile capacity design method for driven piles in sand. In: Proceedings of 4th international symposium on frontiers in offshore geotechnics. Austin, TX, USA, pp 462–477
19. Jardine R, Chow F, Overy R, Standing J (2005) ICP design methods for driven piles in sands and clays. Thomas Telford Ltd., London, UK
20. Fellenius BH (2019) Basics of foundation design. Pile Buck International, Vero Beach, FL, USA
21. Randolph MF, Leong EC, Houlsby GT (1991) One-dimensional analysis of soil plugs in pipe piles. Géotechnique 41(4):587–598
22. Lehane BM, Gavin KG (2001) Base resistance of jacked pipe piles in sand. J Geotech Geoenviron Eng 127(6):473–480

23. Janabi FH, Sakleshpur VA, Prezzi M, Salgado R (2022) Strain influence diagrams for settlement estimation of square footings on layered sand. J Geotech Geoenviron Eng 148(5):04022025
24. Janabi FH, Raja RA, Sakleshpur VA, Prezzi M, Salgado R (2023) Experimental study of shape and depth factors and deformations of footings in sand. J Geotech Geoenviron Eng 149(2):04022128
25. Raja RA, Sakleshpur VA, Prezzi M, Salgado R (2023) Effect of relative density and particle morphology on the bearing capacity and collapse mechanism of strip footing in sand. J Geotech Geoenviron Eng 149(8):04023052
26. Raja RA, Sakleshpur VA, Prezzi M, Salgado R (2023) Load response and soil displacement field for a vertically loaded strip footing on sand underlain by a stiff base. J Geotech Geoenviron Eng 149(11):04023106
27. Arshad M, Tehrani F, Prezzi M, Salgado R (2014) Experimental study of cone penetration in silica sand using digital image correlation. Géotechnique 64(7):551–569
28. Tehrani FS, Han F, Salgado R, Prezzi M, Tovar RD, Castro AG (2016) Effect of surface roughness on the shaft resistance of non-displacement piles embedded in sand. Géotechnique 66(5):386–400
29. Tehrani FS, Arshad MI, Prezzi M, Salgado R (2018) Physical modeling of cone penetration in layered sand. J Geotech Geoenviron Eng 144(1):04017101
30. Tovar-Valencia RD, Galvis-Castro AC, Prezzi M, Salgado R (2018) Short-term setup of jacked piles in a calibration chamber. J Geotech Geoenviron Eng 144(12):04018092
31. Galvis-Castro AC, Tovar-Valencia RD, Salgado R, Prezzi M (2019) Effect of loading direction on the shaft resistance of jacked piles in dense sand. Géotechnique 69(1):16–28
32. Galvis-Castro AC, Tovar-Valencia RD, Salgado R, Prezzi M (2019) Compressive and tensile shaft resistance of nondisplacement piles in sand. J Geotech Geoenviron Eng 145(9):04019041
33. Ganju E, Han F, Prezzi M, Salgado R, Pereira JS (2020) Quantification of displacement and particle crushing around a penetrometer tip. Geosci Front 11(2):389–399
34. Tovar-Valencia RD, Galvis-Castro A, Salgado R, Prezzi M (2021) Effect of base geometry on the resistance of model piles in sand. J Geotech Geoenviron Eng 147(3):04020180
35. Ganju E, Galvis-Castro AC, Janabi F, Prezzi M, Salgado R (2021) Displacements, strains, and shear bands in deep and shallow penetration processes. J Geotech Geoenviron Eng 147(11):04021135
36. Tovar-Valencia RD, Galvis-Castro A, Salgado R, Prezzi M, Fridman D (2023) Experimental measurement of particle crushing around model piles jacked in a calibration chamber. Acta Geotech 18:1331–1351
37. Galvis-Castro AC, Tovar-Valencia RD, Prezzi M, Salgado R (2023) Effect of cyclic loading on the mobilization of unit base resistance of model piles jacked in sand. Acta Geotech 18:4747–4766